THE JOURNAL OF BIOLOGICAL CHEMISTRY VOL. 286, NO. 2, pp. 1618–1626, January 14, 2011

Acute Down-regulation of Sodium-dependent Phosphate Transporter NPT2a Involves Predominantly the cAMP/PKA Pathway as Revealed by Signaling-selective Parathyroid Hormone Analogs[S]

Received for publication, October 28, 2010 Published, JBC Papers in Press, November 3, 2010, DOI 10.1074/jbc.M110.198416

So Nagai[‡], Makoto Okazaki[‡], Hiroko Segawa[‡], Clemens Bergwitz[‡], Thomas Dean[‡], John T. Potts, Jr.[‡], Matthew J. Mahon[‡], Thomas J. Gardella[‡], and Harald Jüppner[‡§1]

From the [‡]Endocrine Unit and the [§]Pediatric Nephrology Unit, Departments of Medicine and Pediatrics, Massachusetts General Hospital and Harvard Medical School, Boston, Massachusetts 02114

The parathyroid hormone (PTH)/PTH-related peptide (PTHrP) receptor (PTHR1) in cells of the renal proximal tubule mediates the reduction in membrane expression of the sodium-dependent P_i co-transporters, NPT2a and NPT2c, and thus suppresses the re-uptake of P_i from the filtrate. In most cell types, the liganded PTHR1 activates $G\alpha_S$/adenylyl cyclase/cAMP/PKA (cAMP/PKA) and $G\alpha_{q/11}$/phospholipase C/phosphatidylinositol 1,4,5-trisphosphate (IP_3)/Ca^{2+}/PKC (IP_3/PKC) signaling pathways, but the relative roles of each pathway in mediating renal regulation P_i transport remain uncertain. We therefore explored the signaling mechanisms involved in PTH-dependent regulation of NPT2a function using potent, long-acting PTH analogs, M-PTH(1–28) (where M = $Ala^{1,12}$, Aib^3, Gln^{10}, Har^{11}, Trp^{14}, and Arg^{19}) and its position 1-modified variant, Trp^1-M-PTH(1–28), designed to be phospholipase C-deficient. In cell-based assays, both M-PTH(1–28) and Trp^1-M-PTH(1–28) exhibited potent and prolonged cAMP responses, whereas only M-PTH(1–28) was effective in inducing IP_3 and intracellular calcium responses. In opossum kidney cells, a clonal cell line in which the PTHR1 and NPT2a are endogenously expressed, M-PTH(1–28) and Trp^1-M-PTH(1–28) each induced reductions in ^{32}P uptake, and these responses persisted for more than 24 h after ligand wash-out, whereas that of PTH(1–34) was terminated by 4 h. When injected into wild-type mice, both M-modified PTH analogs induced prolonged reductions in blood P_i levels and commensurate reductions in NPT2a expression in the renal brush border membrane. Our findings suggest that the acute down-regulation of NPT2a expression by PTH ligands involves mainly the cAMP/PKA signaling pathway and are thus consistent with the elevated blood P_i levels seen in pseudohypoparathyroid patients, in whom $G\alpha_s$-mediated signaling in renal proximal tubule cells is defective.

Parathyroid hormone (PTH),[2] the most important peptide hormone regulator of calcium homeostasis, also contributes importantly to the regulation blood phosphorus levels. These physiologically vital actions of PTH are mediated through the PTH/PTH-related peptide (PTHrP) receptor (PTHR1), which is abundantly expressed in the renal proximal tubules (1, 2). Activation of this G protein-coupled receptor by PTH suppresses the reabsorption of P_i by diminishing protein levels of the sodium-dependent phosphate co-transporter NPT2a, the major phosphate transporter in the renal proximal tubules (3). In addition, PTH regulates the renal type 2c sodium-dependent phosphate co-transporter (NPT2c), as shown by studies in rats rendered hyperphosphatemic by thyroparathyroidectomy, in which exogenous PTH administration causes a marked reduction in the level of NPT2c in renal brush border membrane vesicles (4). This more recently discovered transporter plays a critical role in P_i homeostasis in humans because homozygous or compound heterozygous loss-of-function mutations in *NPT2c* cause hereditary hypophosphatemic rickets with hypercalciuria (5–7).

The OK cell line, which is derived from opossum kidney-proximal tubular cells and thus provides endogenous expression of the PTHR1 and NPT2a, is currently the only genetically non-manipulated cell line for studying PTH-dependent inhibition of phosphate transport (8–10). As in most other cells expressing the PTHR1, stimulation of OK cells with PTH agonists results in the activation of two G protein-dependent signaling pathways, the $G\alpha_s$/adenylyl cyclase/cAMP/PKA (cAMP/PKA) pathway and the $G\alpha_{q/11}$/PLC/IP_3/Ca^{2+}/PKC (IP_3/PKC) pathway. The cumulative data from studies using OK cells (9, 10), other cell-based (11) or animal model systems (12), suggest that both signaling pathways contribute to the PTH-dependent down-regulation of NPT2a expression. The dissection of these signaling pathways in the prior studies has involved the use of PKA and PKC inhibitors and/or the N-terminally truncated fragment PTH(3–34). PTH(3–34) lacks the critical N-terminal residues (Ala^1 and Val^2) required for potent cAMP and IP_3 signaling and thus functions as an antagonist/partial agonist for these pathways (13), whereas it retains the C-terminal residues (Gln^{29}–His^{32}) that, in certain cells, can mediate activation of PKC via an apparent non-PLC-dependent mechanism (14), which could contribute to the PTH-stimulated regulation of NPT2a-dependent phosphate transport.

[S] The on-line version of this article (available at http://www.jbc.org) contains supplemental Figs. S1 and S2.

[1] To whom correspondence should be addressed: Endocrine Unit, Thier 10, 50 Blossum St., Massachusetts General Hospital, Boston, MA 02114. Fax: 617-726-7543; E-mail: hjueppner@partners.org.

[2] The abbreviations used are: PTH, parathyroid hormone; PTHR1, PTH/PTHrP receptor; IP_3, phosphatidylinositol 1,4,5-trisphosphate; OK, opossum kidney; PLC, phospholipase C; PHP, pseudohypoparathyroidism; IBMX, isobutylmethylxanthine; GTPγS, guanosine 5′-3-*O*-(thio)triphosphate.

However, the PLC/PKC-dependent pathway is unable to compensate for the loss or severe impairment of cAMP/PKA signaling in patients with pseudohypoparathyroidism type Ia (PHP-Ia) or type Ib (PHP-Ib). These patients develop PTH-resistant hyperphosphatemia because of maternally inherited mutations that abolish or reduce activity of $G\alpha_s$ in renal proximal tubule cells (15–17). These clinical findings from two related human disorders thus indicate that the cAMP/PKA pathway has a dominant role in the PTH-dependent regulation of NPT2a expression and urinary phosphate excretion, although they do not exclude a contribution of additional signaling mechanisms, such as the IP_3/PKC pathway (11, 12). Thus, despite extensive *in vitro* and *in vivo* investigations, the mechanisms by which PTH mediates the regulation of NPT2a expression and phosphate handling in the proximal renal tubules are not completely understood.

In recent studies on PTH analogs, we identified several new analogs that exhibit unique PTHR1 binding and signaling properties that render them potentially useful for analyzing PTHR1 function *in vitro* and *in vivo*. These analogs, such as M-PTH(1–28) used herein, contain a group of "M" substitutions (M = $Ala^{1,12}$, Aib^3, Gln^{10}, Har^{11}, Trp^{14}, and Arg^{19}) that were initially found to improve the binding affinity of N-terminal PTH fragments by several orders of magnitude (18–20). When extended C-terminally to position 28 or longer, the M-substituted analogs form particularly stable complexes with the PTHR1 and, as a result, induce markedly prolonged cAMP and IP_3 signaling responses in cells, as well as prolonged hypercalcemic and hypophosphatemic responses in mice (21–23). Of note, M-PTH(1–28) lacks the domain that mediates PLC-independent PKC activation, assigned to PTH residues Gln^{29}-His^{32} (24, 25), yet it retains the determinants for potent cAMP and IP_3/Ca^{2+} signaling (Refs. 21–23; and data herein). Importantly, the prolonged effects observed for these analogs *in vivo* are not likely due to altered pharmacokinetic profiles, because the peptides disappear from the circulation at least as rapidly as PTH(1–34) (23). Instead, protracted receptor occupancy, possibly combined with continuous signaling of internalized PTH-PTHR1 complexes, appears to be the mechanism underlying their prolonged actions (26).

Recent studies from others have shown that substitution of Ser or Ala at position 1 in PTH and PTHrP ligands by glycine (13) or bulkier residues, such as benzoylphenylalanine (27) or tryptophan (28), selectively diminish PLC-dependent PKC signaling, with only minor effects on cAMP signaling. As a means to further expand the usefulness of the M-PTH scaffold in dissecting the relative importance of the various signaling pathways in mediating the physiologic effects of PTH, we replaced Ala^1 in M-PTH(1–28) with tryptophan to derive an analog that would potently activate the cAMP signaling pathway but not the PLC/IP_3/Ca^{2+} signaling pathway. Here, we characterize the new analog, Trp^1-M-PTH(1–28), along with its parent, M-PTH(1–28), and use it to further explore the relative roles of the AC/PKA- and PLC/PKC-dependent signaling pathways in mediating the PTH-dependent regulation of NPT2a expression and P_i transport *in vitro* and *in vivo*.

MATERIALS AND METHODS

Peptides—Peptides used were: PTH(1–34) (human sequence: SVSEIQLMHNLGKHLNSMERVEWLRKKLQDVHNF), M-PTH(1–28) (AVAibEIQLMHQHarAKWLNSMRRVEWL-RKKL), Trp^1-M-PTH(1–28) (Ala^1 of M-PTH(1–28) replaced by tryptophan), M-PTH(1–15) (AibVAibEIQLNle-HQHarAKWY), PTH(1–28) (human sequence), rPTH(1–34) (rat sequence with $Nle^{8,21}$ and Tyr^{34} substitutions), and PTH(3–34) (bovine sequence with $Nle^{8,18}$ and Tyr^{34} substitutions). Peptides were C-terminally amidated and synthesized by the Massachusetts General Hospital Biopolymer Core Facility using solid phase, *N*-(9-fluorenyl)methoxycarbonyl (Fmoc)-based chemistry and an automated peptide synthesizer. Peptide purity and authenticity was verified by analytical HPLC and MALDI-mass spectrometry. Radioligands used were ^{125}I-rPTH(1–34) and ^{125}I-M-PTH(1–15), each prepared by chloramine-T-based iodination using ^{125}I-Na (PerkinElmer Life Sciences; specific activity, 2.2 mCi/mmol); the iodinated peptides were purified by reversed phase HPLC.

Cell Cultures—The cell lines used were: African green monkey cell line COS-7; opossum kidney proximal tubule cell line, OK (9, 10); mouse preosteoblastic cell line, MC3T3-E1 (subclone 14, ATCC) (29); and PNEW6, a CHO-derived cell line that is stably transfected to express the rat PTHR1 and NHERF2 (30). The cells were cultured in DMEM (COS-7 and OK) or α-minimum essential medium (MC3T3-E1) supplemented with fetal bovine serum at 10% (COS-7, MC3T3-E1, and PNEW6) or 5% (OK) in an atmosphere of 5% CO_2. The cells were maintained in T-75 flasks and seeded into multiwell plates for DNA transfection and/or assay; the cells were used for analysis 24–72 h after the cell monolayer had reached confluency. COS-7 cells were transiently transfected using FuGENE 6 reagent (Roche Applied Science) and plasmid DNA encoding proteins of interest.

Assays of cAMP and IP_3 Formation—Assays of PTH-dependent cAMP and IP_3 responses were performed at room temperature, as described (22). For cAMP dose-response assays, the cells were incubated with ligand in buffer containing IBMX (2 mM) for 30 min, the buffer was then replaced by 50 mM HCl, and the cAMP content of the lysate was determined by radioimmunoassay. For cAMP "wash-out" assays, the cells were incubated with ligand (1×10^{-7} M) in buffer lacking IBMX for 10 min, and then the cells were rinsed three times and incubated in buffer for varying times. The buffer was then replaced by buffer containing IBMX (2 mM), and incubations were continued for 5 min; the buffer was then replaced by 50 mM HCl, and the intracellular cAMP released in the lysate was quantified by radioimmunoassay. For each ligand and at each wash-out time point, the cAMP levels observed were expressed as percentages of the maximum cAMP responses observed in cells treated for 10 min with ligand in the presence of IBMX (2 mM).

Assays of IP_3 stimulation were performed using PNEW6 cells or COS-7 cells co-transfected with the PTHR1 and $G\alpha_q$. The cells were prelabeled for 18 h with [^{3}H]*myo*-inositol (2 mM; PerkinElmer Life Sciences). At the time of assay, the cells were incubated with ligand in buffer containing LiCl (30 mM)

for 30 min; then the buffer was replaced with an ice-cold solution of 5% trichloroacetic acid; after 30 min, the lysate was neutralized with four volumes of 10 mM Tris, pH 7.4, 2.6 mM NaOH and processed by ion exchange column chromatography using DOWEX-AG1-X8 resin (0.5-ml bed volume). The IP_3 fraction was eluted with 1 M ammonium formate; the eluate was collected into liquid scintillation fluid and counted for ^{3}H-derived β radiation using a Beckman model LS600IC liquid scintillation analyzer.

Binding Assays—The capacities of PTH ligands to bind to two pharmacologically distinct PTHR1 conformational states, called R^0 and RG, which are presumed to reflect populations of G protein-uncoupled and G protein-coupled receptors, respectively, were assessed by competition methods using membranes prepared from transiently transfected COS-7 cells, as described (21, 23). Binding to R^0 was assessed using ^{125}I-rPTH(1–34) as a tracer radioligand, membranes prepared from COS-7 cells transfected with the PTHR1 alone, and the reactions contained GTPγS (10 mM) to promote uncoupling of receptors from heterotrimeric G proteins. Binding to RG was assessed using ^{125}I-M-PTH(1–15) as a tracer radioligand, membranes prepared from COS-7 cells co-transfected with the PTHR1, and a high affinity, dominant-negative $G\alpha_s$ mutant, $G\alpha_s$ND, and the reactions were performed in the absence of GTPγS. Reactions (total reaction volume, 0.2 ml) were conducted in 96-well vacuum filter plates (Multi-Screen system with Durapore HV, 0.65 μM filters; Millipore Corp., Millford, MA) in membrane assay buffer (20 mM HEPES, pH 7.4, 0.1 M NaCl, 3 mM $MgSO_4$, 20% glycerol, 3 mg/ml bovine serum albumin), and a protease inhibitor mixture (Sigma-Aldrich) composed of 4-(2-aminoethyl) benzenesulfonyl fluoride (1 mM final concentration), aprotonin (0.8 μM), leupeptin (20 μM), bestatin (40 μM), pepstatin A (15 μM), and E-64 (14 μM). The reactions contained a total membrane protein concentration of 50 μg/ml and a total radioactivity concentration of ~20,000 cpm/ml. The reactions were incubated for 90 min and terminated by rapid vacuum filtration to separate bound and free radioligand and thorough rinsing of the filter. After air drying, the filters were detached and counted for γ radioactivity using a γ counter. Nonspecific binding was determined in reactions containing unlabeled rPTH(1–34) (3×10^{-7} M). The curves were fit to the data using GraphPad Prism (4.0) software and its sigmoidal dose-response equation.

Measurement of Intracellular Free Calcium (Ca^{2+})—PTH analog effects on Ca^{2+} levels were assessed in PNEW6 cells, which produce a robust Ca^{2+} response to PTH due to exogenous expression of the PTHR1 and NHERF2 (30). Intracellular Ca^{2+} levels were assessed using the cell-permeant fluorescent Ca^{2+} sensor, Fura2-AM (Invitrogen). Cells in a 96-well plate were preloaded with Fura2-AM for 45 min and then unloaded in buffer for 30 min. The plate was then processed using a PerkinElmer Life Sciences Envision plate reader to monitor fluorescence emission at a wavelength (λ_{em}) of 515 nm, upon sequential excitation at wavelengths (λ_{ex}) of 340 and 380 nm. The data were recorded at 2-s intervals for 10 s prior to and for 3 min after ligand addition. The data at each time point were calculated as the ratio of the fluorescence signal obtained with excitation at 340 nm to that obtained with excitation at 380 nm.

P_i Uptake Assay—The uptake of P_i and its inhibition by PTH analogs were assessed, as described (9, 10), in OK cells, which express the opossum orthologs of the PTHR1 and NPT2a. The cells were incubated at 37 °C with ligand (100 nM) for either 4 h (standard assay) or for 10 min followed by a wash-out period in buffer for various times. The cells were then incubated with ^{32}P (PerkinElmer Life Sciences) for 5 min, rinsed thoroughly to remove unincorporated ^{32}P, and then lysed; after adding scintillation fluid, the lysate was counted for ^{32}P-derived β radiation using a Beckman model LS600IC liquid scintillation analyzer.

Determination of Plasma Phosphorous (P_i) Level—Mice (C57BL/6, male; age, 9–12 weeks) were treated in accordance with the ethical guidelines adopted by Massachusetts General Hospital. The mice were injected intravenously via the tail vein with either PTH(1–34), M-PTH(1–28), Trp^1-M-PTH(1–28) (20 nmol/kg), or vehicle (10 mM citric acid, 150 mM NaCl, 0.05% Tween 80, pH 5.0). Tail vein blood was collected immediately prior to and at different times after injection for analysis. Plasma phosphorous was measured using a UV spectroscopic assay (Stanbio Laboratory).

Immunohistochemical Analysis of NPT2a—The mice were injected subcutaneously with a single dose of PTH analogs (50 nmol/kg). After 2 or 6 h, these animals (as well as noninjected, control mice) were infused with ice-cold 4% paraformaldehyde in phosphate buffer before removing the kidneys. After further fixation in the same solution, kidney sections of 5-μm thickness were obtained and incubated with affinity-purified rabbit anti-mouse NPT2a (1:1,000) (kindly provided by Dr. Miyamoto, Tokushima, Japan). Subsequently, the sections were treated with anti-rabbit IgG AlexaFluor-594 and AlexaFluor-488 phalloidine (60 min. at room temperature).

Data Calculations—The curves were fit to the data by nonlinear regression using GraphPad Prism (4.0) software. The data were statistically compared using Student's *t* test, assuming two tails and unequal sample variance (heteroscedastic).

RESULTS

Receptor Binding—The receptor binding properties of M-PTH(1–28) and Trp^1-M-PTH(1–28) as well as the control peptide PTH(1–34) were evaluated by competition methods for binding to two pharmacologically distinct, high affinity states of the PTHR1, R^0 and RG, which, based on their differing sensitivities to GTPγS, are thought to reflect G protein-uncoupled and G protein-coupled receptor conformations, respectively (21, 23). In the R^0 assays, the parent peptide M-PTH(1–28) bound with an apparent affinity that was 12-fold higher than that of PTH(1–34) (Fig. 1*A* and Table 1; $p = 0.0001$), a finding that is fully consistent with our previous studies on this analog (23). The Trp^1-M-PTH(1–28) analog bound to R^0 with an apparent affinity that was ~2-fold weaker than that of M-PTH(1–28) ($p = 0.04$).

In the RG assays, M-PTH(1–28) and Trp^1-M-PTH(1–28), each bound with similarly high apparent affinities of 0.35 and 0.69 nM, respectively (Fig. 1*B* and Table 1; $p = 0.04$). PTH(1–34) bound with an affinity that was severalfold stronger than

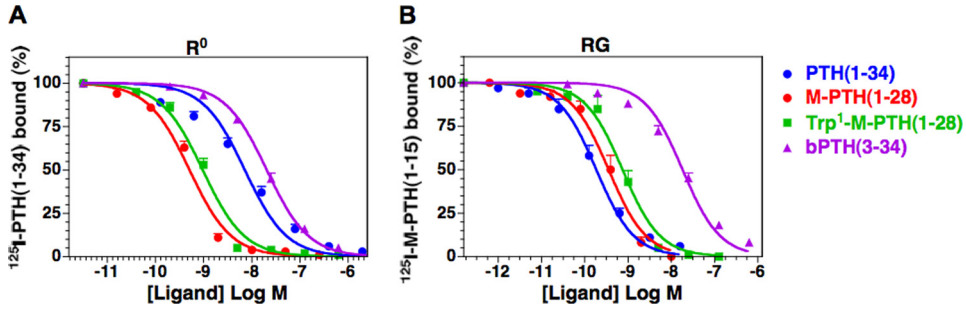

FIGURE 1. **PTH analog binding to the R^0 and RG conformations of the PTHR1.** Binding to the R^0 and RG conformations of the PTHR1 was assessed by competition methods using membranes prepared from COS-7 cells transiently transfected to express the rat PTHR1. *A*, R^0 assays used ^{125}I-rPTH(1–34) tracer radioligand and were performed in the presence of GTPγS. *B*, RG assays used ^{125}I-M-PTH(1–15) tracer radioligand, and the membranes were prepared from cells co-transfected with a high affinity $G\alpha_s$ mutant. The data are the means ± S.E. of five experiments, each performed in duplicate.

TABLE 1
Binding to R^0 and RG PTHR1 conformations

	pIC_{50}	
	R^0	RG
PTH(1–34)	8.17 ± 0.12[a] 6.8[b]	9.86 ± 0.17 0.14
M-PTH(1–28)	9.30 ± 0.08[c] 0.50	9.46 ± 0.20 0.35
Trp¹-M-PTH(1–28)	9.03 ± 0.07[c,d] 0.92	9.16 ± 0.17[e] 0.69
PTH(3–34)	7.70 ± 0.07[a,e] 20	7.80 ± 0.12[a,c] 16

[a] $P < 0.0002$ *versus* M-PTH(1–28).
[b] The values are the nmol of conversion of pIC_{50}. The data are the means ± S.E. ($n = 5$).
[c] $P < 0.001$ *versus* PTH(1–34).
[d] $P < 0.05$ *versus* M-PTH(1–28).
[e] $P < 0.05$ *versus* PTH(1–34).

that of the two modified analogs, but the difference reached significance only for Trp¹-M-PTH(1–28) ($p = 0.02$). The Trp¹ substitution in the M-PTH(1–28) scaffold, therefore, did not severely compromise binding to either the R^0 or RG PTHR1 conformation. In comparing the relative affinities with each analog bound to the two conformations, it can be seen that whereas PTH(1–34) binds with 50-fold stronger apparent affinity to RG, than to R^0, both M-PTH(1–28) and Trp¹-M-PTH(1–28) bind to the two conformations with similar affinities. Thus, the Trp¹-substituted M-PTH(1–28) analog maintains, like its M-PTH(1–28) counterpart peptide, a relatively strong, as compared with PTH(1–34), preference for binding to the R^0 PTHR1 conformation. The antagonist/partial agonist, PTH(3–34), also bound to the R^0 and RG conformations with similar affinities, but in this case, the affinities were ~20-fold weaker than those observed for the modified analogs (Table 1).

cAMP Signaling—The peptides were then evaluated for cAMP signaling potency using the mouse preosteoblastic cell line, MC3T3-E1. The potency of Trp¹-M-PTH(1–28) was 5-fold weaker than that of M-PTH(1–28) (EC_{50}, 0.64 nM *versus* 0.13 nM, respectively, $p = 0.001$) (Fig. 2*A* and Table 2). The maximum responses attained by the two peptides were comparable (~50-fold over basal). PTH(1–34) exhibited a response potency similar to that of M-PTH(1–28), and no cAMP response was detected for PTH(3–34). Similar relative cAMP response activities were seen for the analogs in COS-7 cells expressing the human PTHR1 (supplemental Fig. S1*A*) as well as in OK cells (data below).

The capacities of the ligands to induce persistent signaling responses were assessed by performing wash-out assays in MC3T3-E1 cells (21, 23). In these assays, we treated the cells first with ligand (100 nM) for 10 min and then, at various times after ligand wash-out, with the phosphodiesterase inhibitor IBMX for 5 min. The cAMP content observed in the cells at the end of the treatment was then compared with that observed in cells treated concomitantly with ligand and IBMX for 10 min, set as a maximum of 100% in the analyses. Both M-PTH(1–28) and Trp¹-M-PTH(1–28) induced cAMP responses that were sustained at ~70% of the maximum response level for at least 1 h after ligand addition (Fig. 2*B*); by that time, the response to unmodified PTH(1–28), which binds poorly to R^0 (23), was reduced to ~25% of the maximum value. The response induced by PTH(1–34) was reduced to ~50% of the corresponding maximum cAMP response level by 60 min after wash-out. These data show that the Trp¹-M-PTH(1–28) analog can induce a sustained cAMP response similar to that induced by M-PTH(1–28) and provide further support to the hypothesis that the capacity of a PTH ligand to bind to the R^0 PTHR1 conformation correlates with the duration of the cAMP responses induced by that ligand (21, 23).

IP_3 and Ca^{2+} Signaling—The capacity of the analogs to stimulate IP_3 signaling was then evaluated in PNEW6 cells. These CHO-derived cells are stably transfected to express the rat PTHR1 and NHERF2 and produce robust IP_3 signals in response to PTH and are thus particularly well suited to study activation of the IP_3 signaling pathway by PTH agonists (30). Treatment of these cells with M-PTH(1–28) or PTH(1–34) resulted in ~6-fold increases in intracellular IP_3 (Fig. 2*C* and Table 3). In contrast, Trp¹-M-PTH(1–28) failed to induce an IP_3 response, as did PTH(3–34). In addition, M-PTH(1–28) and PTH(1–34) induced rapid and robust increases in intracellular Ca^{2+} in PNEW6 cells, whereas Trp¹-M-PTH(1–28) induced little or no increase (Fig. 2*D*). As in PNEW6 cells, M-PTH(1–28) induced a 6–8-fold increase in IP_3 levels in COS-7 cells transiently co-transfected to express the human PTHR1 and $G\alpha_q$, whereas little or no increase was observed with Trp¹-M-PTH(1–28) (supplemental Fig. S1*B*). A modest, 4-fold increase in IP_3 accumulation in response to Trp¹-M-PTH(1–28) was observed, however, in COS-7 cells co-transfected to express the rat PTHR1 and $G\alpha_q$, but this response was less efficacious and only ~50% of that attained by

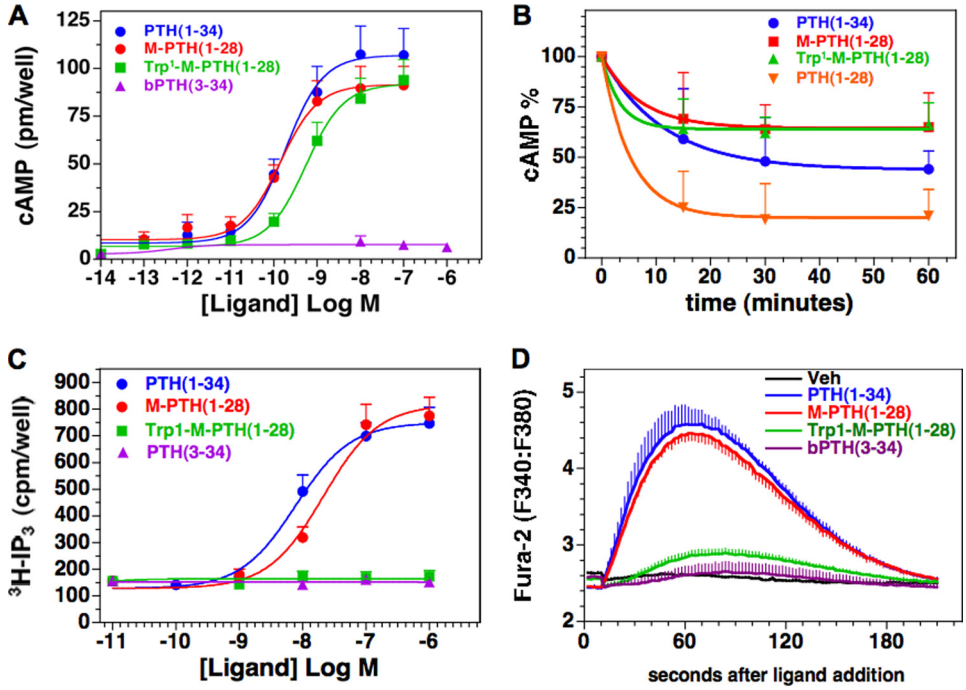

FIGURE 2. **Signaling properties of PTH analogs.** *A*, PTH analogs were assessed at varying doses for the capacity to stimulate cAMP formation in MC3T3-E1 cells. The cells were treated with peptide or buffer control for 30 min at room temperature in the presence of IBMX. The data are the means ± S.E. of seven experiments, each performed in duplicate. *B*, the peptides were also assessed in these cells using a cAMP wash-out assay. For these experiments, the cells were treated with ligand (100 nM) for 10 min in the absence of IBMX, then in buffer alone for the indicated wash-out period, and finally with IBMX-containing buffer for 5 min, and cellular cAMP was measured. The resulting cAMP levels are expressed as a percentage of the maximum cAMP observed in cells treated with peptide (100 nM) for 10 min in the presence of IBMX; these maximum values, set as 100% in the graph, were: PTH(1–34), 97 ± 24 pmol/well; M-PTH(1–28), 102 ± 28 pmol/well; Trp^1-M-PTH(1–28), 82 ± 39 pmol/well; and PTH(1–28), 130 ± 38 pmol/well. The corresponding basal cAMP value was 1.1 ± 0.7 pmol/well. The data are the means ± S.E. of six experiments, each performed in duplicate. *C*, the capacities of the peptides to stimulate the IP_3/Ca^{2+}/PLC/PKC pathway were assessed in PNEW6 cells. Stimulation of IP_3 formation was assessed in cells preloaded with [^{3}H]*myo*-inositol and measuring the cellular accumulation of [^{3}H]inositol trisphosphate following 30 min of ligand treatment. The data are the means ± S.E. of seven experiments, each performed in duplicate. *D*, intracellular calcium responses were assessed in PNEW6 cells preloaded in 96-well plates with the calcium dye Fura2-AM, and the changes were measured as the ratio of fluorescence observed at 515 nm upon excitation at 340 nm to that observed upon excitation at 380 nm. The data are representative of three independent experiments.

TABLE 2
cAMP responses in MC3T3 cells

	pEC_{50}	E_{Max}
		pmol/well
PTH(1–34)	9.68 ± 0.13 0.21[a]	109 ± 14
M-PTH(1–28)	10.0 ± 0.12 0.10	92 ± 10
Trp^1-M-PTH(1–28)	9.28 ± 0.11[b,c] 0.53	93 ± 10
PTH(3–34)	n.d.	17 ± 8[c]
Basal	n.d.	1.9 ± 0.9

[a] The values are the nmol of conversion of pEC_{50}. The data are the means ± S.E. ($n = 7$). n.d., not determined.
[b] $P < 0.05$ *versus* PTH(1–34).
[c] $P < 0.002$ *versus* M-PTH(1–28).

TABLE 3
IP_3 response in PNEW6 cells

	pEC_{50}	E_{Max}
		cpm/well
PTH(1–34)	8.1 ± 0.14 11[a]	705 ± 58
M-PTH(1–28)	7.7 ± 0.07 24	756 ± 90
Trp^1-M-PTH(1–28)	n.d.	148 ± 17
PTH(3–34)	n.d.	144 ± 15
Basal	n.d.	132 ± 2

[a] The values are the nmol of conversion of pEC_{50}. The data are the means ± S.E. ($n = 7$). n.d., not determined.

M-PTH(1–28) or PTH(1–34) (supplemental Fig. S2). These results combined suggest that Trp^1-M-PTH(1–28) is markedly defective, as compared with its parent, M-PTH(1–28), for signaling through the IP_3/Ca^{2+}/PKC pathway yet maintains a potent and prolonged capacity to signal through the cAMP pathway. The signaling properties of Trp^1-M-PTH(1–28) thus differ substantially from those of the N-terminally truncated peptide PTH(3–34), found here to be defective for both PTHR1-mediated cAMP and IP_3/Ca^{2+} signaling. The availability of PTH analogs that activate either the $G\alpha_s$/cAMP/PKA or the $G\alpha_{q/11}$/PLC/Ca^{2+}/IP_3/PKC pathway provided a unique opportunity to further explore which signaling systems are involved in the regulation of NPT2a, the major sodium-dependent phosphate transporter.

PTH Analog Effects on P_i Transport in OK Cells—We compared the capacity of Trp^1-M-PTH(1–28), M-PTH(1–28), and PTH(1–34) to regulate NPT2a function in the OK cell line. First, we assessed the capacity of the ligands to inhibit ^{32}P uptake by these cells using a previously published protocol by which the cells are treated continuously with ligand or buffer control for 4 h, at the end of which the rate of P_i transport is assessed by adding ^{32}P for 5 min and measuring the total radioactivity accumulated in the cells during that 5-min interval. By this protocol, each of the three PTH analogs tested reduced the total phosphate uptake, relative to buffer control,

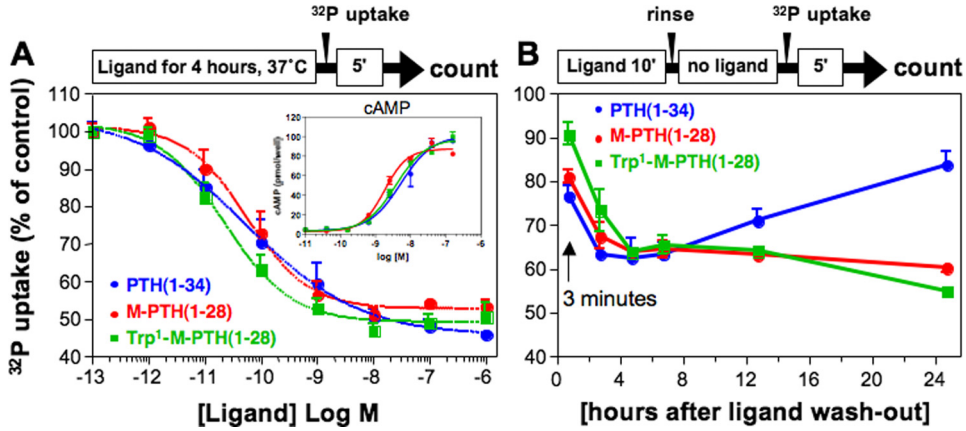

FIGURE 3. **Inhibition of ^{32}P uptake in OK cells.** *A*, PTH analogs were assessed at varying doses for the capacity to inhibit ^{32}P uptake by OK cells. The cells were treated with peptide or buffer control for 4 h at 37 °C, ^{32}P was then added to the cells; after 5 min the cells were rinsed to remove unincorporated ^{32}P, and cell-associated radioactivity was measured after cells lysis. The *inset* shows the accumulation of cAMP, as described for Fig. 2. *B*, the peptides were also assessed in OK cells for their capacity to inhibit ^{32}P uptake using a wash-out assay. The cells were treated with ligand (100 nM) for 10 min, then in buffer alone for the indicated wash-out-period, and finally with ^{32}P-containing buffer for 5 min, before measuring cell-associated radioactivity. The data are the means ± S.E. of three experiments, each performed in duplicate.

to similar extents (~50%) and without significant differences in potencies (EC_{50}, ~0.1 nM; Fig. 3*A*). The comparable efficacies and potencies that the three peptides exhibited for inhibition of P_i uptake were paralleled by similar efficacies and potencies seen for the peptides in cAMP dose-response assays performed in the OK cells (Fig. 3*A*, *inset*).

We then assessed the effects of the ligands on P_i transporter function using a wash-out time course protocol similar to that used in the cAMP time course assays shown in Fig. 1*B*. The cells were thus treated with ligands for 10 min, rinsed to remove unbound ligand, and then incubated for various times in buffer before the addition of ^{32}P for the final 5 min of incubation. The total ^{32}P incorporated into the cell was then assessed as before. As shown in Fig. 3*B*, P_i transport was suppressed to similar extents by the three ligands for the first 6 h after wash-out. In cells treated with PTH(1–34), the rate of P_i uptake had returned close to the initial rate by 24 h after wash-out. In contrast, in cells treated with either M-PTH(1–28) or Trp^1-M-PTH(1–28), the rate of P_i uptake remained suppressed for the entire 24-h wash-out period (Fig. 3*B*). This prolonged suppression of P_i transport could not be explained by a reduction in the viability of the cells or in their general protein functionality, because the levels of trypan blue staining and maximal PTH(1–34)-induced cAMP signaling seen in the treated cells at the end of the 24-hour experiment were similar to those seen in untreated cells (data not shown).

Hypophosphatemic Responses in Wild-type Mice—Our *in vitro* cell-based assays had indicated that substitution of Ala^1 of PTH with the bulkier tryptophan residue blocks PTHR1-mediated IP_3/Ca^{2+} signaling but is permissive for PTHR1-mediated cAMP signaling as well as PTHR1-mediated regulation of P_i transport, thus suggesting that the PLC/IP_3/Ca^{2+}/PKC pathway does not play a critical role in the mechanisms by which PTH down-regulates NPT2a expression or function. To test this hypothesis further, we assessed the capacity of Trp^1-M-PTH(1–28), as compared with M-PTH(1–28) and PTH(1–34), to modulate P_i transporter function *in vivo*. We thus injected mice with either test ligand or vehicle control

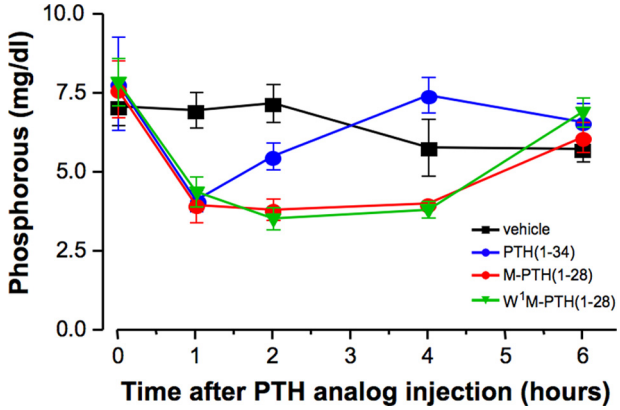

FIGURE 4. **Hypophosphatemic properties of PTH analogs in mice.** Wild-type mice were injected intravenously with vehicle or either PTH(1–34), M-PTH(1–28), or Trp^1-M-PTH(1–28) (each at 20 nmol/kg of body weight); blood was collected from the tail vein to measure plasma phosphorous levels. The data are shown as the means ± S.E. ($n = 4$ for vehicle and PTH(1–34) and $n = 5$ for M-PTH(1–28) and Trp^1-M-PTH(1–28), respectively).

and measured changes in plasma P_i concentrations at varying times after injection. As shown in Fig. 4, relative to the preinjection levels of plasma P_i, each PTH ligand induced a hypophosphatemic response that reached a maximum at 1 h after injection, and the magnitudes of these 1-h responses were similar for the three peptides. In mice treated with PTH(1–34), plasma P_i levels returned to preinjection levels by 4 h, whereas in mice treated with either M-PTH(1–28) or Trp^1-M-PTH(1–28), plasma P_i levels remained maximally suppressed at 4 h and recovered to preinjection levels only by the 6-h time point. Importantly, there was no discernable difference in the effects of the Trp^1-M-PTH(1–28) *versus* M-PTH(1–28) analogs on plasma P_i levels.

Immunohistochemical Analysis of the Kidneys of PTH-treated Animals—We next examined directly the effects of the ligands on the expression of NPT2a in the kidney using immunohistochemical methods. In mice injected with vehicle, abundant NPT2a staining was observed at the apical, brush border membrane of the proximal tubular cells (Fig. 5). In mice injected with PTH(1–34), there was a dramatic reduc-

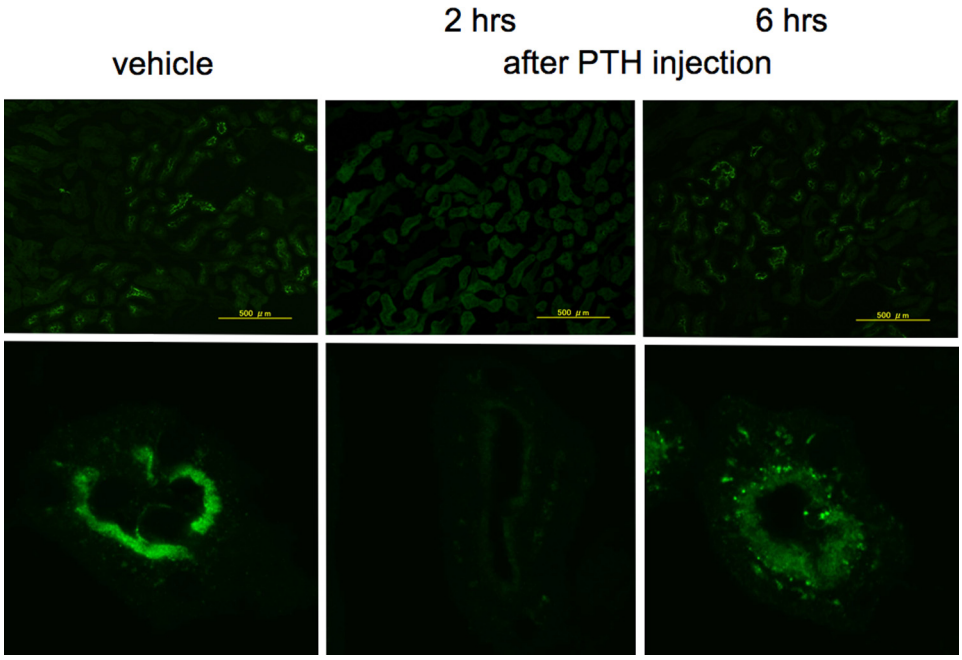

FIGURE 5. **Effect of PTH(1–34) on Npt2a expression in mice.** Wild-type mice were injected subcutaneously with a single dose of PTH(1–34) (50 nmol/kg of body weight). 2 and 6 h after the injection, the kidneys were removed, sectioned, and immunostained for Npt2a expression (see "Materials and Methods"). Staining was compared with that observed with noninjected mice. Magnification, ×100 in the *upper panels* and ×2000 in the *lower panels*.

tion, relative to vehicle, in the level of NPT2a staining at the apical surface by 2 h after injection, with a partially recovery of surface staining by 6 h. Thus, the prolonged hypophosphatemic effects observed for M-PTH(1–28) and Trp^1-M-PTH(1–28) could be explained by a prolonged reduction in the surface expression level of the NPT2a transporter on the apical surface of renal proximal tubule cells (Fig. 6).

DISCUSSION

The activated PTHR1 stimulates the formation of several different second messengers. The PTH analog M-PTH(1–28) showed *in vitro* potent activation of the cAMP/PKA and IP_3/Ca^{2+}/PKC pathways, with at least the former response being prolonged (not testable for the latter), and it was previously shown to have potent *in vivo* effects on bone and calcium homeostasis (21, 23, 26). Its position 1-modified variant, Trp^1-M-PTH(1–28), showed *in vitro* a similarly potent and prolonged activation of the cAMP/PKA pathway, yet it was clearly defective for activation of the IP_3/$[Ca^{2+}]_i$/PKC pathway. This defect in IP_3 signaling was even apparent in COS-7 cells overexpressing $G\alpha_q$, which are thus maximized for agonist-activated formation of IP_3, when expressing the human PTHR1. There was a significant IP_3 response observed in COS-7 cells overexpressing $G\alpha_q$ and the rat PTHR1 (supplemental Fig. S2), and a small and less efficient increase in intracellular free Ca^{2+} upon stimulation with Trp^1-M-PTH(1–28) was observed in PNEW6 cells (rat PTHR1). Both of these responses, however, were much reduced when compared with that of M-PTH(1–28) or PTH(1–34). The signaling selectivity of the Trp^1 analog provided a unique opportunity to investigate which signaling pathway downstream of the liganded PTHR1 is most prominently involved in the acute regulation of renal phosphate handling.

In studying OK cells, which naturally express the marsupial orthologs of PTHR1 and NPT2a but not the marsupial ortholog of NPT2c, we showed that M-PTH(1–28), Trp^1-M-PTH(1–28), and PTH(1–34) have similar efficacy for stimulating the accumulation of the second messenger cAMP and for reducing the uptake of phosphate, at least when using the established protocol of a 4-h ligand incubation. However, using a short term exposure of cells to the three ligands revealed marked differences. The inhibitory effect of PTH(1–34) started to wane at 4 h after the initial 10-min exposure to this ligand. In contrast, the inhibitory effects of M-PTH(1–28) and Trp^1-M-PTH(1–28) persisted for more than 24 h, and it took more than 3 days before phosphate uptake was again comparable with that observed in untreated OK cells (data not shown). These findings suggest that prolonged signaling through the cAMP/PKA pathway by both PTH analogs contributes strongly to their prolonged inhibitory effects on phosphate transport in OK cells.

Consistent with these *in vitro* findings, M-PTH(1–28) and Trp^1-M-PTH(1–28) showed, in comparison with PTH(1–34), much prolonged hypophosphatemic activity when injected intravenously into wild-type mice. These data are consistent with findings in OK cells where short term treatment with either M-PTH(1–28) or Trp^1-M-PTH(1–28) resulted in a more complete down-regulation of NPT2a expression than did treatment with PTH(1–34). Moreover, our finding that both M analogs were equally potent *in vivo* despite their marked differences in IP_3 signaling *in vitro* leads us to conclude that the IP_3/PKC pathway is not prominently involved in the acute regulation of NPT2a expression.

The findings in humans affected by pseudohypoparathyroidism type Ia or type Ib are consistent with this conclusion.

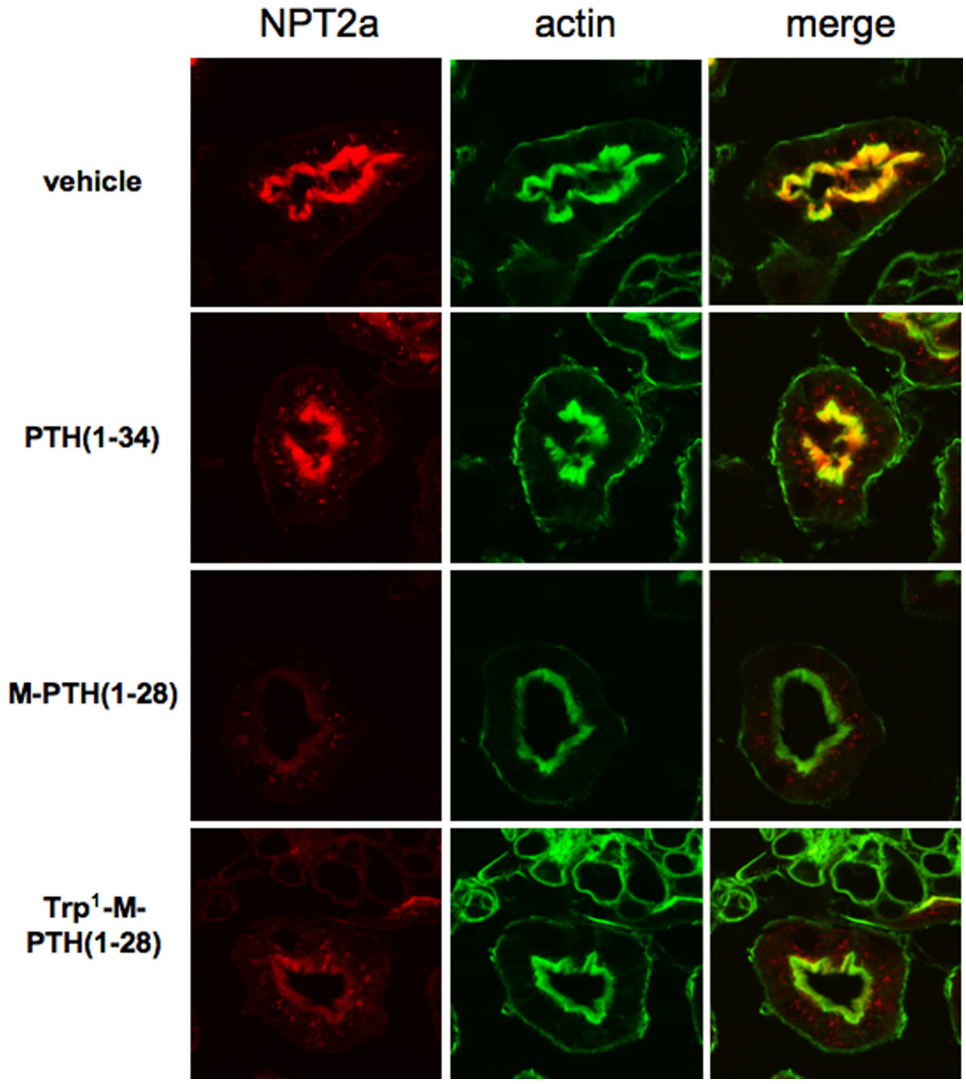

FIGURE 6. **Effect of PTH analogs on Npt2a expression in mice.** The animals were injected subcutaneously with a single dose of PTH(1–34), M-PTH(1–28), or Trp^1-M-PTH(1–28) (50 nmol/kg of body weight). 6 h after the injection, the kidneys were removed, sectioned, and immunostained for Npt2a and actin expression (see "Materials and Methods"). Prolonged reduction of NPT2a expression in wild-type mice treated with M-PTH(1–28) and Trp^1-M-PTH(1–28).

PHP-Ia is caused by maternally inherited loss-of-function mutations in those *GNAS* exons that encode $G\alpha_s$, and PHP-Ib is caused by maternally inherited microdeletions within or upstream of *GNAS*, which result in loss of methylation at *GNAS* exon A/B and reduced expression of $G\alpha_s$ (17). In the proximal renal tubules where $G\alpha_s$ appears to be expressed only from the maternal allele, the heterozygous mutations identified in patients with PHP-Ia or PHP-Ib thus lead to an absent or severely blunted increase in urinary cAMP excretion after PTH application (15–17). The blunted phosphaturic response to injection of PTH in these patients is most easily explained by a lack of cAMP/PKA-dependent signaling and, hence, an insufficient PTH-mediated reduction in NPT2a expression. In contrast to the impaired acute phosphaturic response to PTH, which is likely cAMP/PKA-dependent, a delayed PTH-induced increase in urinary phosphate excretion was previously observed in patients with pseudohypoparathyroidism (presumably type Ia) (31). This delayed response to PTH may involve cAMP/PKA-independent signaling events affecting the expression of NPT2a or other phosphate transporters such as NPT2c, which appears to be less rapidly regulated by PTH (4). In any case, these additional mechanisms to increase urinary phosphate excretion appear to be insufficient to normalize serum phosphate levels in patients affected by PHP-Ia and PHP-Ib.

In conclusion, taking advantage of long acting, signaling selective PTH analogs, we were able to show *in vitro* that NPT2a is primarily regulated through cAMP/PKA-dependent mechanisms. Furthermore, IP_3/PKC-deficient (Trp^1-M-PTH(1–28)) and IP_3/PKC-sufficient (M-PTH(1–28)) PTH analogs induced equivalent phosphaturic responses in mice, thus providing *in vivo* evidence for the conclusion that NPT2a is regulated predominantly, at least acutely, through cAMP/PKA-dependent signaling mechanisms. Because of their pharmacological characteristics, long acting PTH analogs may be particularly useful for the treatment of patients with acquired or congenital forms of hypoparathyroidism.

REFERENCES

1. Gardella, T. J., Jüppner, H., Brown, E. M., Kronenberg, H. M., and Potts, J. T., Jr. (2010) in *Endocrinology* (DeGroot, L. J., and Jameson, J. L., eds)

6th Ed., pp. 1040–1073, W. B. Saunders, Philadelphia, PA
2. Lupp, A., Klenk, C., Röcken, C., Evert, M., Mawrin, C., and Schulz, S. (2010) *Eur. J. Endocrinol.* **162,** 979–986
3. Tenenhouse, H. S. (2007) *J. Steroid Biochem. Mol. Biol.* **103,** 572–577
4. Segawa, H., Yamanaka, S., Onitsuka, A., Tomoe, Y., Kuwahata, M., Ito, M., Taketani, Y., and Miyamoto, K. (2007) *Am. J. Physiol. Renal Physiol.* **292,** F395–F403
5. Bergwitz, C., Roslin, N. M., Tieder, M., Loredo-Osti, J. C., Bastepe, M., Abu-Zahra, H., Frappier, D., Burkett, K., Carpenter, T. O., Anderson, D., Garabedian, M., Sermet, I., Fujiwara, T. M., Morgan, K., Tenenhouse, H. S., and Jüppner, H. (2006) *Am. J. Hum. Genet.* **78,** 179–192
6. Lorenz-Depiereux, B., Benet-Pages, A., Eckstein, G., Tenenbaum-Rakover, Y., Wagenstaller, J., Tiosano, D., Gershoni-Baruch, R., Albers, N., Lichtner, P., Schnabel, D., Hochberg, Z., and Strom, T. M. (2006) *Am. J. Hum. Genet.* **78,** 193–201
7. Ichikawa, S., Sorenson, A. H., Imel, E. A., Friedman, N. E., Gertner, J. M., and Econs, M. J. (2006) *J. Clin. Endocrinol. Metab.* **91,** 4022–4027
8. Jankowski, M., Hilfiker, H., Biber, J., and Murer, H. (2001) *Kidney Blood Press Res.* **24,** 1–4
9. Cole, J. A., Eber, S. L., Poelling, R. E., Thorne, P. K., and Forte, L. R. (1987) *Am. J. Physiol.* **253,** E221–E227
10. Cole, J. A., Forte, L. R., Eber, S., Thorne, P. K., and Poelling, R. E. (1988) *Endocrinology* **122,** 2981–2989
11. Mahon, M. J., Cole, J. A., Lederer, E. D., and Segre, G. V. (2003) *Mol. Endocrinol.* **17,** 2355–2364
12. Forster, I. C., Hernando, N., Biber, J., and Murer, H. (2006) *Kidney Int.* **70,** 1548–1559
13. Takasu, H., Baba, H., Inomata, N., Uchiyama, Y., Kubota, N., Kumaki, K., Matsumoto, A., Nakajima, K., Kimura, T., Sakakibara, S., Fujita, T., Chihara, K., and Nagai, I. (1996) *Endocrinology* **137,** 5537–5543
14. Whitfield, J. F., Isaacs, R. J., Chakravarthy, B., Maclean, S., Morley, P., Willick, G., Divieti, P., and Bringhurst, F. R. (2001) *J. Bone Miner. Res.* **16,** 441–447
15. Jan de Beur, S. M., and Levine, M. A. (2001) in *The Parathyroids: Basic and Clinical Concepts* (Bilezikian, J. P., Markus, R., and Levine, M. A., eds) pp. 807–825, Academic Press, New York
16. Weinstein, L. S., Yu, S., Warner, D. R., and Liu, J. (2001) *Endocr. Rev.* **22,** 675–705
17. Bastepe, M., and Jüppner, H. (2005) *Horm. Res.* **63,** 65–74
18. Shimizu, M., Carter, P. H., Khatri, A., Potts, J. T., Jr., and Gardella, T. J. (2001) *Endocrinology* **142,** 3068–3074
19. Shimizu, M., Shimizu, N., Tsang, J. C., Petroni, B. D., Khatri, A., Potts, J. T., Jr., and Gardella, T. J. (2002) *Biochemistry* **41,** 13224–13233
20. Shimizu, N., Dean, T., Khatri, A., and Gardella, T. J. (2004) *J. Bone Miner. Res.* **19,** 2078–2086
21. Dean, T., Linglart, A., Mahon, M. J., Bastepe, M., Jüppner, H., Potts, J. T., Jr., and Gardella, T. J. (2006) *Mol. Endocrinol.* **20,** 931–943
22. Dean, T., Vilardaga, J. P., Potts, J. T., Jr., and Gardella, T. J. (2008) *Mol. Endocrinol.* **22,** 156–166
23. Okazaki, M., Ferrandon, S., Vilardaga, J. P., Bouxsein, M. L., Potts, J. T., Jr., and Gardella, T. J. (2008) *Proc. Natl. Acad. Sci. U.S.A.* **105,** 16525–16530
24. Jouishomme, H., Whitfield, J. F., Chakravarthy, B., Durkin, J. P., Gagnon, L., Isaacs, R. J., MacLean, S., Neugebauer, W., Willick, G., and Rixon, R. H. (1992) *Endocrinology* **130,** 53–60
25. Jouishomme, H., Whitfield, J. F., Gagnon, L., Maclean, S., Isaacs, R., Chakravarthy, B., Durkin, J., Neugebauer, W., Willick, G., and Rixon, R. H. (1994) *J. Bone Miner Res.* **9,** 943–949
26. Ferrandon, S., Feinstein, T. N., Castro, M., Wang, B., Bonley, R., Potts, J. T., Jr., Gardella, T. J., and Vilardaga, J. P. (2009) *Nat. Chem. Biol.* **10,** 734–742
27. Bisello, A., Chorev, M., Rosenblatt, M., Monticelli, L., Mierke, D. F., and Ferrari, S. L. (2002) *J. Biol. Chem.* **277,** 38524–38530
28. Gesty-Palmer, D., Chen, M., Reiter, E., Ahn, S., Nelson, C. D., Wang, S., Eckhardt, A. E., Cowan, C. L., Spurney, R. F., Luttrell, L. M., and Lefkowitz, R. J. (2006) *J. Biol. Chem.* **281,** 10856–10864
29. Wang, D., Christensen, K., Chawla, K., Xiao, G., Krebsbach, P. H., and Franceschi, R. T. (1999) *J. Bone Miner. Res.* **14,** 893–903
30. Mahon, M. J., Donowitz, M., Yun, C. C., and Segre, G. V. (2002) *Nature* **417,** 858–861
31. Bell, N. H., Avery, S., Sinha, T., Clark, C. M., Jr., Allen, D. O., and Johnston, C., Jr. (1972) *J. Clin. Invest.* **51,** 816–823